JOURNAL OF MATERIALS SCIENCE 19 (1984) 3437–3442

Particle condensation in metallic vapour plumes

E. R. BUCKLE, K. J. A. MAWELLA, D. J. HITT
Condensation Laboratory, Department of Metallurgy, The University, Sheffield, UK

An apparatus is described for the study of aerosol particle condensation in a plume of vapour rising from a heated source. The principal advantages of this plume chamber over the heat-pulse cloud chamber previously used include the attainment of steady-state conditions at a controlled source temperature and the suppression of recirculation. The coagulation of particles and the further growth or re-evaporation that tends to occur in the outer zone of the heat-pulse equipment is discouraged, and samples taken on substrates positioned in the plume are expected to be more representative of the original nucleation and growth processes.

Aerosol particles were condensed in zinc vapour emitted at various source temperatures (T_0) with the walls at room temperature (T_∞). Trends occur in particle size and morphology when T_0 is varied at fixed T_∞ which broadly resemble those in the cloud chamber work, where T_∞ is varied. Thus, in addition to the dendrites and prisms typical of low T_0 there is an increasing proportion of spheres when T_0 is raised above the melting point, until they eventually become the only species present. The particles condensing in the invisible fume generated at T_0 settings below the melting point, were found to consist only of prisms and dendrites. This confirms that these particles condense directly in the solid state, unlike the spheres, which are originally liquid. The trends observed when changing T_0 at constant T_∞ are shown to be in agreement with theoretical predictions for nucleation in a boundary layer.

1. Introduction

Metallurgical fumes produced by evaporation and natural condensation contribute greatly to the accumulation of particles in the atmosphere, and a better understanding of condensation mechanisms is required if attempts to modify or suppress the fumes at source are to be successful. Detailed studies on the aerosols produced in the heat-pulse cloud chamber have already been reported [1–3]. In those experiments the nucleation and growth of aerosols in vapours emitted into a stagnant gas-filled enclosure were investigated for various settings of the sink, or wall, temperature (T_∞). The source temperature (T_0) was pulsed to induce the nucleation of discrete clouds rather than a continuous fume. In the work, carried out at atmospheric pressure, it was found that the density of clouds and the characteristics of the particles settling from them depended closely on T_∞. Over a similar period a considerable body of results on fume generated in a closed vessel under reduced pressure has been reported by other research groups (e.g. [4, 5]).

For theoretical purposes, there is a need to study more specifically the effects of different source temperatures, as well as sink temperatures, on nucleation and particle development. In addition, the production of particles in flowing gases is more pertinent to many industrial situations than a closed chamber method. Even in a flow system, however, care must be taken to avoid complications resulting from the recirculation of old particles into the vapour near the source. It was with this in mind that a new apparatus was designed that additionally allowed the natural development of an evaporation plume resembling the steady emission of a horizontal, one-dimensional source. The present paper describes

0022–2461/84 $03.00 + .12 © *1984 Chapman and Hall Ltd.*

the new "plume chamber" and its application to a study of the growth of metallic fume particles when the vapour is emitted into a flow of cool, inert gas.

2. Design and operation of plume chamber

Relevant laboratory-scale work on the stability of laminar convection plumes as well as our own experience on aerosol condensation was taken into consideration in the design of the apparatus. The aim was to be able to generate vapour continuously from a line source into a laminar, upward flow of supporting gas, avoiding stagnation and recirculation.

A schematic diagram of the complete apparatus is given in Fig. 1. The chamber consists of two coaxial glass chimneys, of i.d. 6.82 and 9.44 cm, respectively, of which the internal chimney functions as the plume chamber proper. A self-supporting Perspex throat, positioned in the internal chimney above the source and restricting the diameter of the flow to 3.13 cm, is effective in stabilizing the plume against the tendency to sway and break up. It does this by inhibiting the recirculation of turbulent gas [6–8].

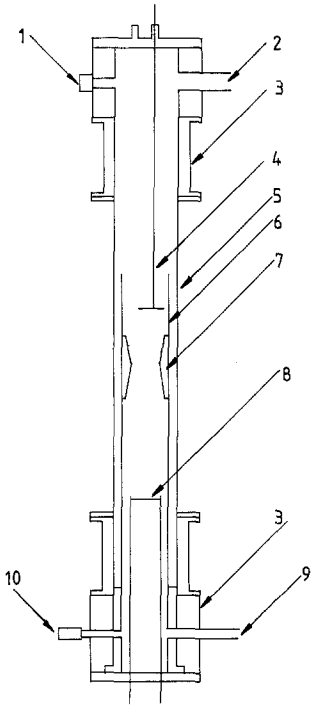

Figure 1 Diagram of plume chamber. 1, vacuum release valve; 2, gas outlet; 3, supporting blocks; 4, sampling probe; 5, external chimney; 6, internal chimney; 7, Perspex throat; 8, boat; 9, gas inlet; 10, vacuum gauge.

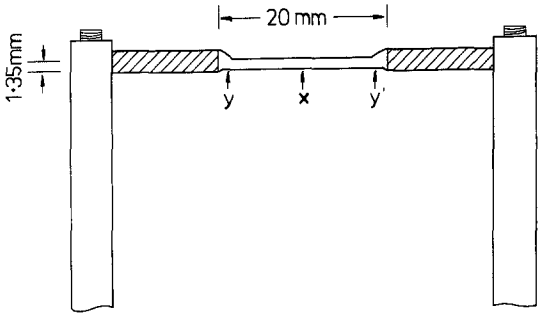

Figure 2 Stainless steel heating boat and supporting conductors. x, position of thermocouple junction; y y', positions of leads for measurement of voltage drop.

The specimen of test substance in the form of 1 mm wire is contained in a hemi-cylindrical boat, 16 mm long and cut from 1.35 mm diameter thin-wall stainless-steel tubing. The ends of the boat are pinched into slots in the robust supporting conductors (Fig. 2). A.c. power is supplied to the conductors via a mains Variac and a stepdown transformer in order to heat the boat and its contents. The source temperature, T_0, which can be varied by adjusting the power input, is measured by a thermocouple spot-welded to the underside of the boat opposite the sample. A measure of the power dissipated in the boat and contents at fixed current can be obtained by recording the voltage drop between two leads welded to the ends of the hollow section of the boat. A two-channel chart recorder is used to follow the temperature of the thermocouple and the boat voltage drop simultaneously during a fuming run.

Fig. 3 is typical of a chart record so obtained, and shows the trends of temperature and voltage in response to a fixed power setting. In the presence of the volatile metal specimen the temperature rises rapidly to point p, where there is a momentary melting arrest commencing with a sharp peak. It then continues to rise to point q, the beginning of the volatilization arrest. At sufficiently high power settings this is also the point at which fume first becomes visible. During this second arrest the temperature rises only slowly, but at the end of fuming (point r), when the specimen has completely evaporated, it rapidly proceeds to the final, steady value characteristic of the power and gas flow settings (point s). The temperature at s is reached more directly in a run without the volatile specimen (dashed curve in Fig. 3).

The response curve for voltage is similar, but

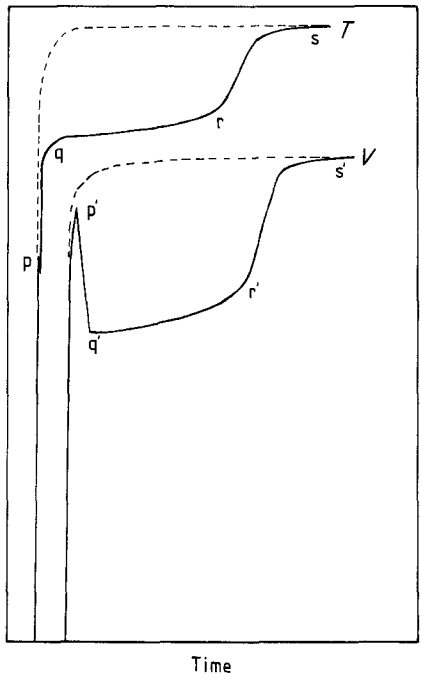

Figure 3 Temperature (T) and voltage (V) response curves at fixed boat power. Dashed lines: control runs with no volatile charge in boat.

the temperature arrest at the melting point is represented by a large peak preceding the volatilization arrest (point p′). If the melted specimen wets the boat (as is the case with zinc) it becomes part of the electrical heating circuit, and the resistance of the boat section is lowered with a consequent fall in boat voltage. The point q′ now represents the onset and point r′ the termination of fuming. Finally, the voltage rises after evaporation to point s′, characteristic of the empty boat.

In experiments aimed at the study of fuming at fixed source temperature the procedure is to switch on the power at the level necessary to achieve the required temperature at point q. In such tests the run is stopped by switching off the power while the temperature is still in the arrest q–r.

To sample particles in the plume a probe is lowered into it from the top of the chimney. This probe carries a number of gold-coated silica substrates for SEM examination and carbon-coated copper grids for TEM examination. The substrates may be positioned in either the upward or downward-facing direction (Fig. 4). The probe shaft enters the apparatus through an "O"-ring seal, allowing the distance between the source and

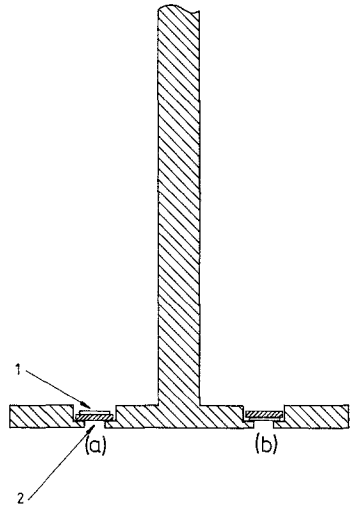

Figure 4 Detail of sampling probe with substrates facing (a) upward, (b) downward. (1) copper grid, (2) glass support.

the substrates to be varied as well as the position in the horizontal plane.

3. Experiments with zinc

The chamber was evacuated and flushed with high-purity argon before a plume was formed in order to displace air. Two flow speeds of the supporting gas, 1 and 2 cm sec^{-1}, were used in the experiments, it having been established in previous trials that at these settings plug flow was achieved in the absence of heating. The charge of zinc (99.99% purity) was a 5 mm length of 1 mm diameter wire. In the main series of runs the source temperatures used to generate fume at each flow speed were: 673, 754, 918, 962, 1083 and 1213 K at 1 cm sec^{-1} and 858, 985, 1033 and 1173 K at 2 cm sec^{-1}. The particles were collected by mounting the substrates at 22.5 cm above the source, the throat being at 14.5 cm above the source (Fig. 1). To minimize oxidation the sampled particles were quickly transferred to a coating unit and covered with a thin layer of evaporated carbon. Philips EM301 and EM400 electron microscopes were used to examine the deposits.

4. Results

The small difference between the flow-speed settings had no significant influence on the characteristics of the particles. This indicates that no serious disturbance of the laminar flow pattern set up by the inert gas resulted from the generation of vapour and that the results of repeat experiments

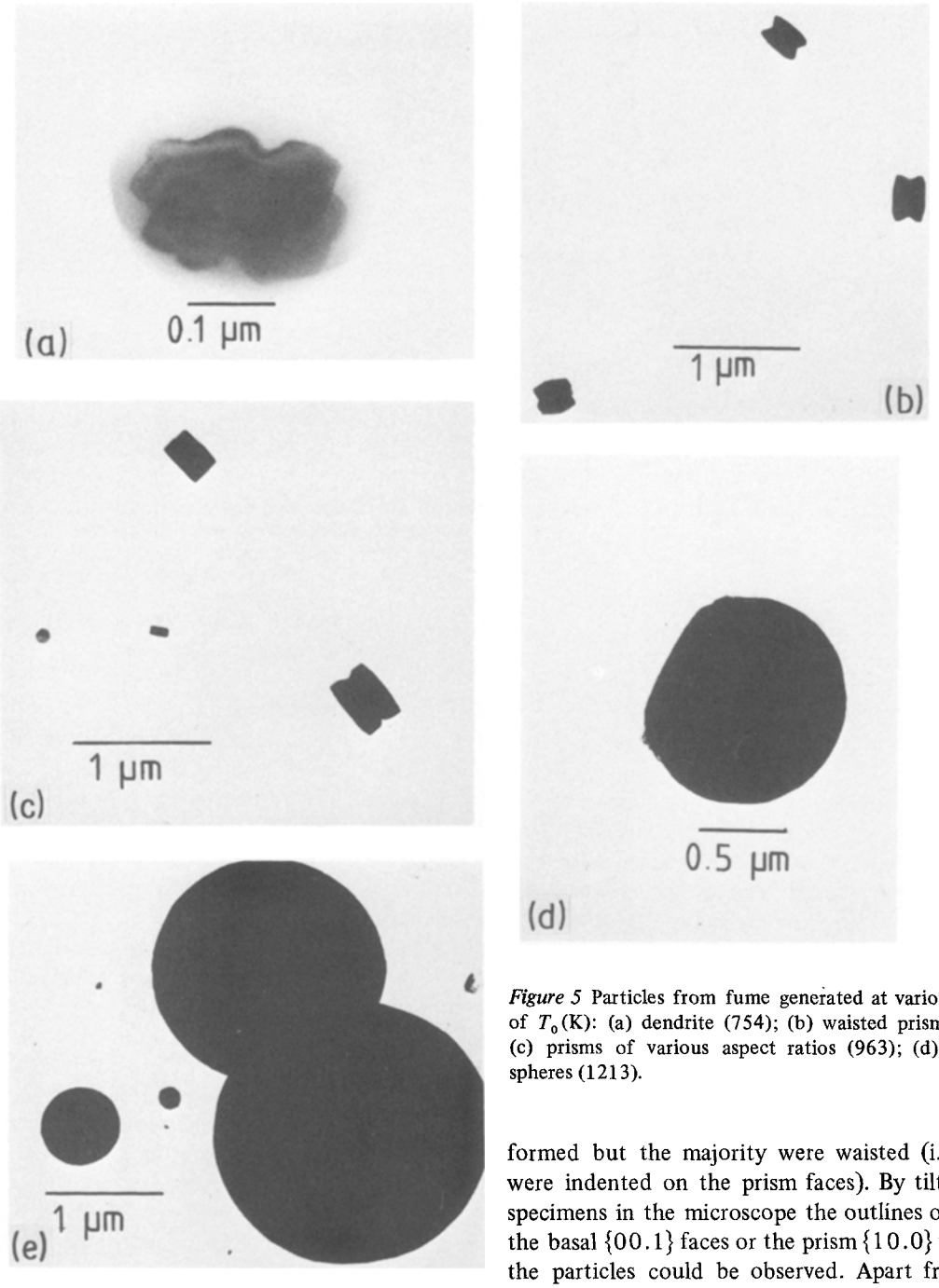

Figure 5 Particles from fume generated at various values of T_0(K): (a) dendrite (754); (b) waisted prisms (918); (c) prisms of various aspect ratios (963); (d) and (e) spheres (1213).

in the new apparatus could be expected to be identical.

A noticeable alteration in particle morphology was found as T_0 was increased. At the lowest settings (673 and 754 K) the fume was invisible and the specimen grids were only sparsely populated with dendrites and prisms. Some prisms were well formed but the majority were waisted (i.e. they were indented on the prism faces). By tilting the specimens in the microscope the outlines of either the basal {00.1} faces or the prism {10.0} faces of the particles could be observed. Apart from the prisms, the dendrites from which they originate were represented only by forms in which the radiating arms were substantially fused in the basal areas. No spherical particles occurred at these source temperatures. A dendritic particle generated at 754 K in argon flowing at 1 cm sec^{-1} is shown in Fig. 5a.

Fumes generated at intermediate temperatures (858 and 918 K) were visible and deposited mostly

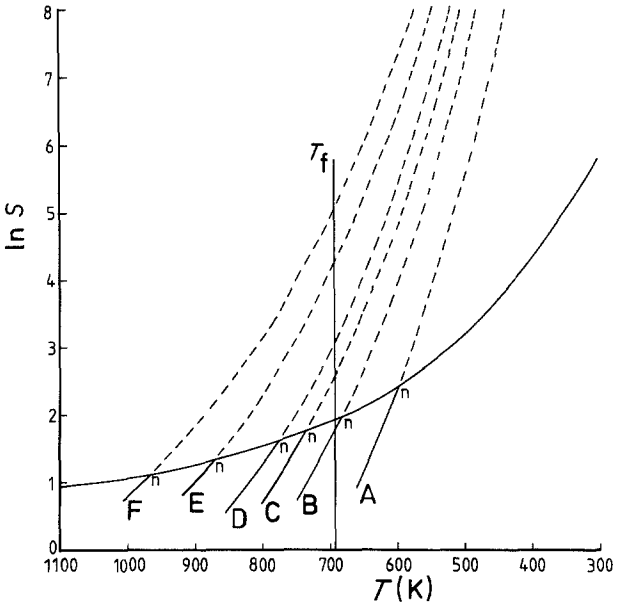

Figure 6 Amelin diagram showing positions of nucleation thresholds (n) in zinc vapour evaporating from a source at various temperatures (T_0) into an unreactive atmosphere at 300 K and 1 bar. T_0 (K): (A) 700; (B), 800; (C) 850; (D) 900; (E) 1000; (F) 1100. The unlabelled curve gives the temperature profile of S^*.

prisms but some spheres. At 918 K there were more waisted prisms than well-formed ones (Fig. 5b), and the spheres tended to be larger than the prisms, although the two forms also occurred in comparable sizes.

As T_0 was further increased, the proportion of waisted prisms decreased in favour of the well-formed kind. Most of the prisms were larger than those found with lower T_0 although the shape was also affected, some "thin" particles of unusually large aspect ratio [9] also being present. Fig. 5c, which shows particles collected with a source temperature of 963 K and gas speed of 1 cm sec^{-1}, illustrates this.

Among the particles generated at 1033 K spheres were predominant. Not only was the proportion of prisms greatly reduced; they were now consistently smaller than spheres. In fact, it appears that after an initial increase in size with increasing T_0, setting prisms become smaller again as T_0 rises further.

At still higher T_0, fume particles consisted mainly of comparatively large spheres; only a few small prisms were seen. The outlines of the spheres showed the presence of the basal flats identified by Buckle and Pointon [2] as the vestiges of floating rafts. Not more than one raft was visible at a time (Fig. 5d), suggesting that the spheres were monocrystalline over the whole range of source temperatures. Figs. 5d and e are typical of the samples generated at 1213 K and 1 cm sec^{-1}.

5. Discussion

The change from a prismatic to a spherical particle morphology suggests a change in condensation mechanism. Such a change of mechanism was inferred from similar evidence of morphological variation when aerosols of certain metallic salts were condensed at various settings of the *sink* temperature T_∞ [10]. The possibility of a change in condensation mechanism has also been discussed by Buckle and Pointon [11].

Results of theoretical calculations on nucleation of aerosols in boundary layers were presented by Buckle and Tsakiropoulos [3]. In this approach nucleation theory is used to test the possibility that the temperature and concentration profiles across the boundary layer over an evaporating surface could support nucleus formation, without going into the question of the sizes to which the nuclei eventually grow. The broad conclusions of such an approach can be used to interpret the change in particle morphology with increasing *source* temperature, as now observed. The plume chamber has the advantage over the heat-pulse cloud chamber in that T_0 is known as well as T_∞ [11].

The situation in the boundary layer over zinc evaporating at various source temperatures into an unreactive gas at a sink temperature well below the melting point (694 K) is illustrated in the Amelin diagram of Fig. 6. In this diagram, the supersaturation ratio, S, of vapour is plotted against the

decreasing local temperature in the evaporation–condensation boundary layer after the manner of Amelin [12]. The resulting Amelin profile is shown for various T_0 (curves A to F in Fig. 6). The curve of critical supersaturation ratio, S^*, derived from nucleation theory (unlabelled curve) for a nucleation rate of 1 $m^{-3} sec^{-1}$ is superimposed on the Amelin profiles. This value for the nucleation rate may be taken as an arbitrary measure of the threshold of nucleation. Since the curve of S^* is intersected by every Amelin profile, the diagram predicts that nucleation is to be expected at all values of T_0.

The morphology of the fume particles first nucleated will, however, depend on the temperature at the point of intersection, designated n in Fig. 6. The first-formed nuclei will grow into liquid or solid condensate according to the position of the contact temperature, T_n, in relation to the melting point, T_f. At relatively low source temperatures, T_n will lie below T_f and all nuclei will grow directly into solid particles. This deduction is confirmed by the occurrence of prisms and dendrites and the absence of spheres at low source temperatures such as 673 and 754 K. It is shown in Fig. 6 that even at a source temperature of 800 K the Amelin profile intersects the curve for S^* at a temperature below T_f.

At higher source temperatures point n is moved further to the left, and at some stage T_n reaches T_f. It is to be expected that this marks the beginning of liquid-phase nucleation.

However, the profile of the Amelin curve beyond the point where the temperature has fallen to T_n (dashed lines in Fig. 6) cannot be predicted without allowing for the growth of the nuclei. It is possible, for example, that nucleation could continue for some distance *beyond* point n. If T_n were not too high, the vapour on passing T_f would produce nuclei of solid particles. The resulting fume would consist of a mixture of particles grown from solid and liquid nuclei. In this way the presence of both prismatic and spherical particles in the fume evolved at intermediate T_0 settings may be accounted for.

As the source temperature is raised still further, nucleation of the vapour to the liquid would be expected to take over, with, eventually, the formation only of spherical particles. Although in the experiments efforts were made to bring the temperature of the source to the chosen level as fast as possible, so as to obtain a characteristic crop of particles in the fume sample, supersaturation appears to have occurred briefly at low temperatures during the run-up, resulting in the formation of a few prisms. In view of their small size, notwithstanding their early nucleation, such prisms evidently fail in the competition with spheres for vapour.

Acknowledgements

The authors acknowledge support from the Department of Trade and Industry (Warren Spring Laboratory) and the Science and Engineering Research Council during the period of this work.

References

1. E. R. BUCKLE and K. C. POINTON, *J. Mater. Sci.* **10** (1975) 365.
2. *Idem, ibid.* **12** (1977) 75.
3. E. R. BUCKLE and P. TSAKIROPOULOS, Proceedings International Conference on Environmental Pollution, Thessaloniki, 21–25 September 1981, edited by A. Anagnostopoulas (The University of Thessaloniki, Thessaloniki, 1981) p. 375.
4. R. UYEDA, *J. Crystal Growth* **45** (1978) 485.
5. C. KAITO, *Jap. J. Appl. Phys.* **17** (1978) 601.
6. R. J. FORSTROM and E. M. SPARROW, *Int. J. Heat. Mass Transfer* **10** (1967) 321.
7. A. W. SCHORR and B. GEBHART, *ibid.* **13** (1970) 557.
8. T. FUJI, I. MORIAKA and H. UEHARA, *ibid.* **16** (1973) 755.
9. E. R. BUCKLE and P. TSAKIROPOULOS, *J. Mater. Sci.* **14** (1979) 1421.
10. E. R. BUCKLE and C. N. HOOKER, *Trans. Faraday Soc.* **58** (1962) 1939.
11. E. R. BUCKLE and K. C. POINTON, *Faraday Disc. Chem. Soc.* **61** (1976) 92.
12. A. G. AMELIN, "Theory of Fog Condensation", translated by Z. Lerman (IPST, Jerusalem, 1976).

Received 6 January
and accepted 24 January 1984